Remediation of lead-contaminated water by virgin coniferous wood biochar adsorbent: batch and column application

Maria Rosaria Boni[1], Agostina Chiavola[1], Simone Marzeddu[1]*

[1] Faculty of Civil and Industrial Engineering, Department of Civil, Constructional and Environmental Engineering (DICEA), Sapienza University of Rome, Via Eudossiana 18, 00184 Rome, Italy.
* Correspondence: simone.marzeddu@uniroma1.it; Tel.: +39 06 44585514.

Abstract

In this paper, RE-CHAR® biochar, produced by a wood biomass pyrolysis process, which is usually applied as a soil fertilizer, was investigated for a novel use, that was as adsorbent for remediating a lead-contaminated solution. Firstly, a deep physical and chemical characterization of RE-CHAR® biochar was carried out. Then, the adsorption capacity of lead from 50 mg/L and 100 mg/L solutions was determined under batch and continuous flow conditions. Kinetics of the batch adsorption process were very rapid and complete removal was achieved within 4 h contact time at both Pb concentrations, using a biochar dosage of 5 g/L. These data were best fitted by the pseudo second-order model, with the rate constant and the equilibrium capacity equal to k_s = 0.0091 g/min and q_e = 9.9957 mg/g at 50 mg/L Pb, and k_s = 0.0128 g/min and q_e = 20.1462 mg/g at 100 mg/L Pb, respectively. The Langmuir isotherm model best fitted the equilibrium data at both Pb concentrations, with the Langmuir constant and maximum adsorption capacity equal to: b = 11.5804 L/mg and q_{max} = 4.6116 mg/g at 50 mg/L Pb, and b = 2.8933 L/mg and q_{max} = 9.5895 mg/g at 100 mg/L Pb. Continuous flow column tests showed that adding biochar to the soil of the adsorbent bed significantly extended the breakthrough and exhaustion times, with respect to the column filled with soil only. The Thomas model best fitted the experimental data of the breakthrough curves, with the constant $k_{TH} = 5.28 \times 10^{-5}$ mL/min·mg and the maximum adsorption capacity q_0 = 334.57 mg/g which was comparable to the values reported for commercial adsorbents.

Based on these results, it can be assessed that RE-CHAR® biochar can be used as an effective adsorbent for lead removal from water solutions even at high concentrations.

Key words: adsorption; batch; biochar; column; lead; remediation.

1. Introduction

Charcoals (or biochars) are produced by means of the thermal decomposition of organic residues from different sources, conducted under controlled conditions of the oxidizing agent (Basu 2010; Glaser 2007; Popa and Visa 2017). In particular, biochar can be obtained by the pyrolysis process of biomasses (Hagemann et al. 2018; Kan et al. 2016; J. Li et al. 2016) or vegetable waste from agriculture and forestry (Joseph et al. 2017; Keske et al. 2019; Yargicoglu et al. 2015). Furthermore, it is generated as a residue of the gasification process (Lugato et al. 2013; Rollinson 2016; Yao et al. 2018).

Quality and properties of the biochar depend on many factors, such as feedstock type and operating conditions of the production process (Ahmed et al. 2016a; Allaire et al. 2015; Aller 2016; Lange et al. 2018; Tang et al. 2013; Tripathi et al. 2016; K. Weber and Quicker 2018). Table 1 shows the impact of parent materials and production process conditions on the elemental composition and surface area of biochar (Chen et al. 2008; Jindo et al. 2014; Kong et al. 2011; Mašek et al. 2012; Nguyen et al. 2009, 2010; Uchimiya et al. 2011).

Table 1. Influence of feedstock and production process conditions on surface area and elemental composition of biochar.

Feedstock type	**Reactor**	**Temperature** °C	**Residence time** h	**Heating rate** °C/min	**C** (%)	**O** (%)	**BET Surface area** m^2/g	**Ref.**
Apple tree branch (AB)	Commercial electric furnace	400-800	10	10	70.18 – 84.84	20.56 –5.81	11.90– 545.43	(Jindo et al. 2014)
Oak tree (OB)	Commercial electric furnace	400-800	10	10	70.52 – 82.85	21.47 – 17.29	5.60– 398.15	(Jindo et al. 2014)
	Slow pyrolizer	350-600	n.d	n.d	n.d.	n.d.	450 - 642	(Nguyen et al. 2010)
Rice husk (RH)	Commercial electric furnace	400-800	10	10	44.59 – 40.41	16.32 – 2.69	193.70 – 295.57	(Jindo et al. 2014)
	Gold image furnace	350, 450, 550 and 650	n.d.	5 and 100	66.14 – 89.61	57.2	29.19 – 7.64	(Mašek et al. 2012)
Rice straw (RS)	Commercial electric furnace	400-800	10	10	49.92 – 29.17	12.02 – 3.71	46.60 – 256.96	(Jindo et al. 2014)
Pine wood chips (PC)	Gold image furnace	350, 450, 550 and 650	n.d.	5 and 100	69.64 – 87.89	44.7	26.58 – 8.29	(Mašek et al. 2012)
Pine needle	Pyrolizer	100-700	6	n.d.	50.87 – 86.51	42.27 – 11.08	0.65 – 490.8	(Chen et al. 2008)
Wheat	Gold	350, 450,	n.d.	5 and	70.88	53.1	21.96	(Mašek

Feedstock type	**Reactor**	**Temperature** °C	**Residence time** h	**Heating rate** °C/min	**C** (%)	**O** (%)	**BET Surface area** m^2/g	**Ref.**
straw (WS)	image furnace	550 and 650		100	– 94.90		– 0.00	et al. 2012)
Cotton seed hulls	Box furnace	200-800	4	n.d.	51.9 - 90	40.5 - 7	4.7 - 322	(Uchimiya et al. 2011)
Corn stover	Slow pyrolizer	350-600	n.d	n.d	n.d.	n.d.	293 - 527	(Nguyen et al. 2009)
Soybean stalk	Muffle furnace	300, 400, 500, 600 and 700	8	n.d	n.d	n.d.	144.14 – 250.23	(Kong et al. 2011)

Currently, biochar is mainly used as a soil amendment due to the capacity of improving its properties and quality (Lomaglio et al. 2018; Schmidt et al. 2014). Agegnehu et al. (2017) observed an increase of soil pH from 7.1 to 8.1 as a consequence of the addition of 39 t/ha herbaceous biochar. Glaser et al. (2002) reported that low amounts of biochar added to soils (i.e. 300 g/kg) increased the availability of base cations (ECEC) (i.e. above 4.8 $cmol_c/kg$) and base saturation (BS) (i.e. above 660%). Mean soil organic carbon content (SOC), after 67 days, increased between 5.1 and 14.2 g/kg, with the addition of 1-2% biochar to Norfolk Ap soil (Novak et al. 2009). Burrel et al. (2016) disclosed the change in the value of electrical conductivity (EC) of soils amended with 3% biochar for 3 years, of different soil types: for instance, a decrease of about 37 $\mu S\ cm^{-1}$ was observed in planosol soil, whereas an increase of about 25 $\mu S\ cm^{-1}$ was measured in černozëm and cambisol soil. In a review of several studies

conducted at different scales (laboratory, field, field plots, greenhouse), Blanco-Canqui (2017) reported that, in the upper 15 cm of soils depth, bulk density decreased of at least 10% while porosity increased at the same percentage. Plant growth and health showed different responses in relation to the biochar source and application rate. In the review of crops responses (mainly maize and tomato) by Agegnehu et al. (2017), it was highlighted an increase of plant growth yield of 50% on average. Application of biochar to soil can also reduce nutrient leaching by increasing the soil retention capacity and stimulate the growth rate of microorganisms (Jien et al. 2017; Rasa et al. 2018). For instance, Hagemann et al. (2017) observed 2.0 g NO_3^--N/kg after 60 days of aerobic composting plus 6 months of storage. Bashir et al. (2018) measured 224.13 mg/kg of microbial mass carbon (MBC) in a soil amended with 1.5% sugarcane bagasse-derived biochar. Thanks to the high heterogeneous specific surface (Kasozi et al. 2010) and the well-distributed pore network that includes micropores (<2 nm), mesopores (2–50 nm) and macropores (>50 nm), biochar showed also to possess a high ion exchange capacity, such as $10 \leq CEC \leq 69$ $cmol_c/kg$ at near neutral pH as reported by Mukherjee et al. (2011).

Due to the these properties, biochar was tested as adsorbents for the removal of pollutants from different environmental compartments (Ahmad et al. 2014; Cha et al. 2016; De Gisi et al. 2016; Qian et al. 2015; Rosales et al. 2017; Wei et al. 2018). In water and wastewater, it was capable of adsorbing a wide range of pollutants such as lead, arsenic, copper, cadmium, chromium, mercury, zinc and nickel (Ahmad et al. 2014; De Gisi et al. 2016; Z. Ding et al. 2016; M. I. Inyang et al. 2016; Mohan et al. 2007; Oliveira et al. 2017; Qambrani et al. 2017; Reddy et al. 2014; Xiao fei Tan et al. 2016; Xiaofei Tan et al. 2015). Biochar was also applied to the remediation of groundwater contaminated by slow-release secondary sources (Luciano et al. 2010; Tatti et al. 2016, 2019).

Adsorption capacity was further enhanced through different activation processes, such as biological, thermal or physical-chemical (Boni et al. 2018a; Z. Ding et al. 2016; R. Li et al. 2017; Rajapaksha et al. 2016; B. Wang et al. 2017; H. Wang et al. 2015; Wei et al. 2018). Biochar was dosed to contaminated soils with the aim to reduce pollutant leaching (Bashir et al. 2018; Beesley et al. 2011, 2014; Lomaglio et al. 2018; K. Lu et al. 2017; Park et al. 2011; Puga et al. 2015; Tang et al. 2013; Yin et al. 2016; Zhang et al. 2016). When incorporated to soil, it demonstrated to be capable of binding heavy metals to carbonates and organic matter: as a consequence, the adsorption process was enhanced due to metals building bonds with oxygen, carbon and nitrogen-containing functional groups (Bashir et al. 2018; Cha et al. 2016; Lehmann et al. 2011; Park et al. 2011; Yin et al. 2016). In addition, the high pH, Cation Exchange Capacity (CEC), microporous structure and excess of soluble salts, which are present on the biochar surface, increase the heavy metal immobilization through precipitation and surface adsorption (Beesley et al. 2011; Febrianto et al. 2009; Janus et al. 2015; Sohi et al. 2010; Uchimiya et al. 2010, 2011; Vithanage et al. 2017; B. Wang et al. 2017; M. Wang et al. 2017).

As compared to commercial adsorbents, use of biochar represents a more economically and environmentally sustainable alternative because it offers a new opportunity of reuse to vegetable products and green wastes from agriculture and forestry. Therefore, its employment fully fits the goals of the circular economy which require to limit waste materials by their recovery and reuse. Furthermore, using biochar in place of commercial adsorbents allows to avoid the environmental impact of the industrial activities required for their production.

Lead is one of the most studied toxic substances. It negatively affects almost all vertebrate systems and also human health through drinking water ingestion (Abadin et al. 2007; Flora et al. 2012; Wani et al. 2015). Due to the associated risks (Cobbina et al. 2013; Hanna-Attisha et al. 2016), Italian legislation requires Pb concentration to be below 0.01

mg/L in groundwater, 0.2 mg/L and 0.3 mg/L in the effluents discharged into surface waters and sewage systems, respectively (Italian decree n. 152/06).

Several technologies have been developed to remove lead and other heavy metals from the environment thus preventing it from spreading. For instance, different types of adsorbents have been applied to contaminated soils and water to reduce/immobilize, metal content such as talc, chalcopyrite and barite (Rashed 2001), soil-washing agents (Neilson et al. 2003), activated red mud (Naga Babu et al. 2017), sophorolipids (Qi et al. 2018), nanoadsorbent from different sources (Chiavola et al. 2016; Safatian et al. 2019).

In this study, a virgin coniferous wood biochar produced in Italy was tested as adsorbent for removing lead from aqueous solutions. To this purpose, a number of experimental trials was carried out in laboratory to evaluate the adsorption capacity under both batch and continuous flow conditions.

The novelty of the present paper is represented by the new application of virgin coniferous wood biochar as adsorbent media for lead-contaminated solution in batch and column plants. This paper demonstrates the feasibility of a different use for this waste product, thus allowing to comply with the basic principles of the circular economy.

2. Materials and methods

2.1. Production of biochar

RE-CHAR®, supplied by RECORD IMMOBILIARE S.r.l. (Lunano, Italy), is produced from a wood biomass (virgin coniferous wood, mainly pine) through a pyrolyzation process conducted under the following operating conditions: 600 °C average gasification temperature, 750 °C effluent gas temperature and 300 °C inlet air temperature. The pyrolysis plant aimes at enery production, and generates biochar as a solid residue product. Currently, this biochar is

used as a soil improver for which it has received the Italian certification (0019841/17, decree 75/2010 "*reorganization and revision of the rules on soil improvers"*).

The wood biomass used as a feedstock is produced by the forest management activities and is composed by wood chips having a particle size distribution predefined by a mechanical treatment. Feedstock complies with the A1/A2 quality classes of the UNI EN ISO 17225-4: 2014 standard.

Due to processing issues, broad-leaved wood chips from coppice are also used along with wood chips, in a mixture of oak, orniello and hornbeam. As far as the production process is concerned, the biomass is transported from the storage tank to the drying phase through mechanical systems using rakes and augers; here, the water content is reduced to about 10% through the insufflation of 8000 m^3/h hot air by means of the Air Handling Unit (AHU). Then, the biomass suitable for gasification is selected through sieving, and automatically loaded to the plant where it undergoes a thermochemical conversion in an oxygen deficient environment.

2.2. Analytical methods

Prior to be used, RE-CHAR® was chemically and physically characterized according to standard procedures reported in previous published papers (Qambrani et al. 2017). Particularly, bulk density, specific weight, field capacity, porosity, moisture content, ash content and pH were determined following the analytical procedures outlined by Allaire et al. (2015) and Pituello et al. (2015). The value of pH point of zero charge was measured by applying the method reported in Noh and Schwarz (1990). Elemental analysis of the surface (EDX), percentage of the major components and average dimension of pores were determined by using a HR FESEM Zeiss Auriga (SEM; Rome, Italy) at 3000× magnification and 10 kV acceleration voltage.

159 Lead concentration in the aqueous phases was determined using a Perkin Elmer atomic
160 absorption spectrophotometer with flame atomization (F-AAS; Perkin-Elmer model 3030B),
161 whose detection limit was 0.1 mg/L. The calibration curve was determined using standard
162 solutions at 2 mg/L and 4 mg/L Pb (APAT and IRSA/CNR 2003). Samples were properly
163 diluted using the relative method (APAT and IRSA/CNR 2003) to fall within the instrument's
164 calibration curve.

165 **2.3. Chemical solutions**

166 A stock solution (at 30 g/L Pb^{2+}) was prepared by dissolving lead(II) nitrate salt (supplied
167 by Carlo Erba, Milan, Italy; solubility in water = 52 g/100 mL, at 20 ± 0.1 °C) into Milli-Q
168 water (18.5 MΩ·cm).

169 Proper dilutions of the stock solution in deionized water (0.055 μS/cm) allowed to obtain
170 the lead contaminated solutions at the required concentrations (i.e. 50 mg/L and 100 mg/L)
171 for the experimental tests. Stock and lead-contaminated solutions were stored at 4°C until
172 their use.

173 **2.4. Batch tests**

174 Batch experiments were carried out, using the jar-tester apparatus, to determine kinetics
175 and equilibrium data of the adsorption process of lead onto the RE-CHAR® biochar. The
176 experiments were conducted at 50 and 100 mg/L of lead as initial concentrations. These
177 values, being very high and far above the limits posed by the Italian legislation, were selected
178 with the aim to test the adsorption capacity of the biochar under severe contamination
179 conditions (Kołodyńska et al. 2017).

180 In the batch tests, 5 g/L of biochar were added to the Pb-contaminated solution and
181 maintained for 6 h under mixing conditions at 120 rpm constant stirring speed. Liquid
182 samples were collected at different times: 5, 15, 30, 45 and 60 min within the first hour, and
183 afterwards at 1 h intervals until the end of the tests. The samples were filtered by a vacuum

184 filtration system using a 0.2 μm glass microfibre filters (Munktell, Ahlstrom) and then the
185 liquid phase was analyzed.

186 Through the above batch tests, it was possible to determine the equilibrium time of the
187 adsorption process. The experimental data were fitted using the following kinetic models:
188 zero, first, second, saturation, pseudo-first and pseudo-second-order (Sirini 2002). The best
189 fitting model between the experimental and the modelled data was determined based on the
190 value of the regression coefficient, R^2, using the linearized form of the model equations.

191 Another series of batch tests was conducted with the aim of obtaining the equilibrium
192 data. In this case, the following adsorbent dosages of RE-CHAR® were added to the solutions
193 at 50 and 100 mg/L Pb concentrations: 0.5, 1, 2, 4, 5, 6, 8 and 10 g/L. The content was
194 maintained under mixing conditions for a duration equal to the equilibrium time previously
195 determined.

196 At the end of these tests, liquid samples were collected, filtered by a vacuum filtration
197 system using a 0.2 μm glass microfibre filters (Munktell, Ahlstrom) and analyzed for the
198 residual Pb concentration in solution.

199 The equilibrium data were fitted by the Langmuir (Langmuir 1918), Freundlich
200 (Freundlich 1907) and Brunauer–Emmett–Teller (BET) (1938) isotherm models. The best
201 fitting model of the experimental data was determined based on the value of R^2, using the
202 linearized form of the model equations.

203 Lead percentage removal (R%), lead adsorbed per unit weight of adsorbent at time t (q_t)
204 and at equilibrium time (q_e) were calculated using the following equations (1, 2, and 3,
205 respectively), obtained through the mass balance of lead between the liquid and solid phases:
206

$$R\% = \frac{(C_0 - C_t)}{C_0}\ 100\% \qquad (1)$$

$$q_t = \frac{(C_0 - C_t)V}{m} \quad (2)$$

$$q_e = \frac{(C_0 - C_e)V}{m} \quad (3)$$

where V is the volume of the aqueous solution, m is the mass of RE-CHAR®, C_0 (equal to 50 and 100 mg/L Pb), C_t and C_e indicate lead concentration in the liquid phase at time t = 0, t and at equilibrium, respectively.

All the batch experiments were conducted in duplicate and the results obtained were averaged.

2.5. Column tests

The adsorption capacity of biochar in a column plant was investigated using a lab-scale apparatus. These tests were performed following the procedures outlined in a previous paper by the same authors (Boni et al. 2018a). For instance, glass columns, having 18 cm height and 1 cm diameter, were filled by alternating layers of sand, soil and biochar. Particularly, a previously sterilized quartz sand was placed on the bottom; 1 g of agricultural soil (made by 29% clay, 28% silt, 43% sand and 2% organic matter, by weight) was posed above, followed by a layer of RE-CHAR® disposed on the top.

The mass of biochar used in the column test, equal to 0.5 g, was selected according to the procedure previously determined by the same authors (Boni et al. 2018b).

Biochar and sand particle having a size smaller than 2 mm were previously discarded, in order to limit by-pass phenomena along the column walls (Perry and Green 2008). One more column, filled as the previous one but without the the layer of RE-CHAR®, was operated under the same conditions as a control.

The lead contaminated solution, at a concentration C_0 = 100 mg/L Pb, was continuously fed to the top of the columns through peristaltic pumps, at 60 mL/h flow rate. This high

concentration of lead was chosen to test the RE-CHAR® adsorption capacity under severe conditions, and to obtain a rapid development of the breakthrough curve.

By recording Pb concentrations in the eluates versus column operating time allowed to determine the breakthrough curves. Then, the breakthrough and saturation times were calculated, assuming to correspond to the time when Pb concentrations in the eluate, C, corresponds to C/C_0 = 5% and C/C_0 = 95%, respectively (Chern and Chien 2002; Hai et al. 2018).

The experimental data of the column tests were fitted using the Yoon–Nelson (1984), Thomas (1944) and Bohart–Adams (1920) models (Ahmed et al. 2016b; Bhaumik et al. 2013) to determine the adsorption capacity.

3. Results and discussion

3.1. Biochar characterization

Values of the main chemical-physical properties of RE-CHAR® were determined through the characterization phase conducted as described in section 2.3. The results obtained are shown in Table 2.

Table 2. Main physical and chemical properties of RE-CHAR® (% on dry weight).

Physical and Chemical Properties	Symbol	Unit	Values
Bulk density	γ_s	g/cm^3	1.931
Specific weight	γ_d	g/cm^3	0.167
Field capacity	ω_c	g in 100 g	700
Porosity	n	%	91.35
Carbon	C	%	92.56

Oxygen	O	%	5.87
Calcium	Ca	%	0.81
Potassium	K	%	0.53
Magnesium	Mg	%	0.18
Moisture content	ω	%	2.94
Ash content	cc	%	56.87
Potential of Hydrogen	pH	-	12.40
Point of zero charge	pH_{PZC}	-	12.98

Characterization provided values in accordance to those reported by the specialized literature. For instance, carbon and oxygen contents were found equal to 92.6% and 5.9%, respectively, whereas Qambrani et al. (2017) measured C = 93.7% and O = 5.8% in a biochar produced from turkey litter pine needle pyrolyzed at 700 °C. The ash content was found to be 56.9% in the present case, likely a direct effet of the high pyrolysis temperature (600 °C). In a recent study by other authors, the ash content of biochar produced from swine manure was observed to be about 53%, being the pyrolysis temperature equal to 700 °C (Klasson 2017).

The Scanning Electron Microscope (SEM) images of RE-CHAR® surface are shown in Figure 1, at various magnifications: (A) 79 X; (B) 2.50 KX; (C) 2.00 KX; and (D) 100.00 KX.

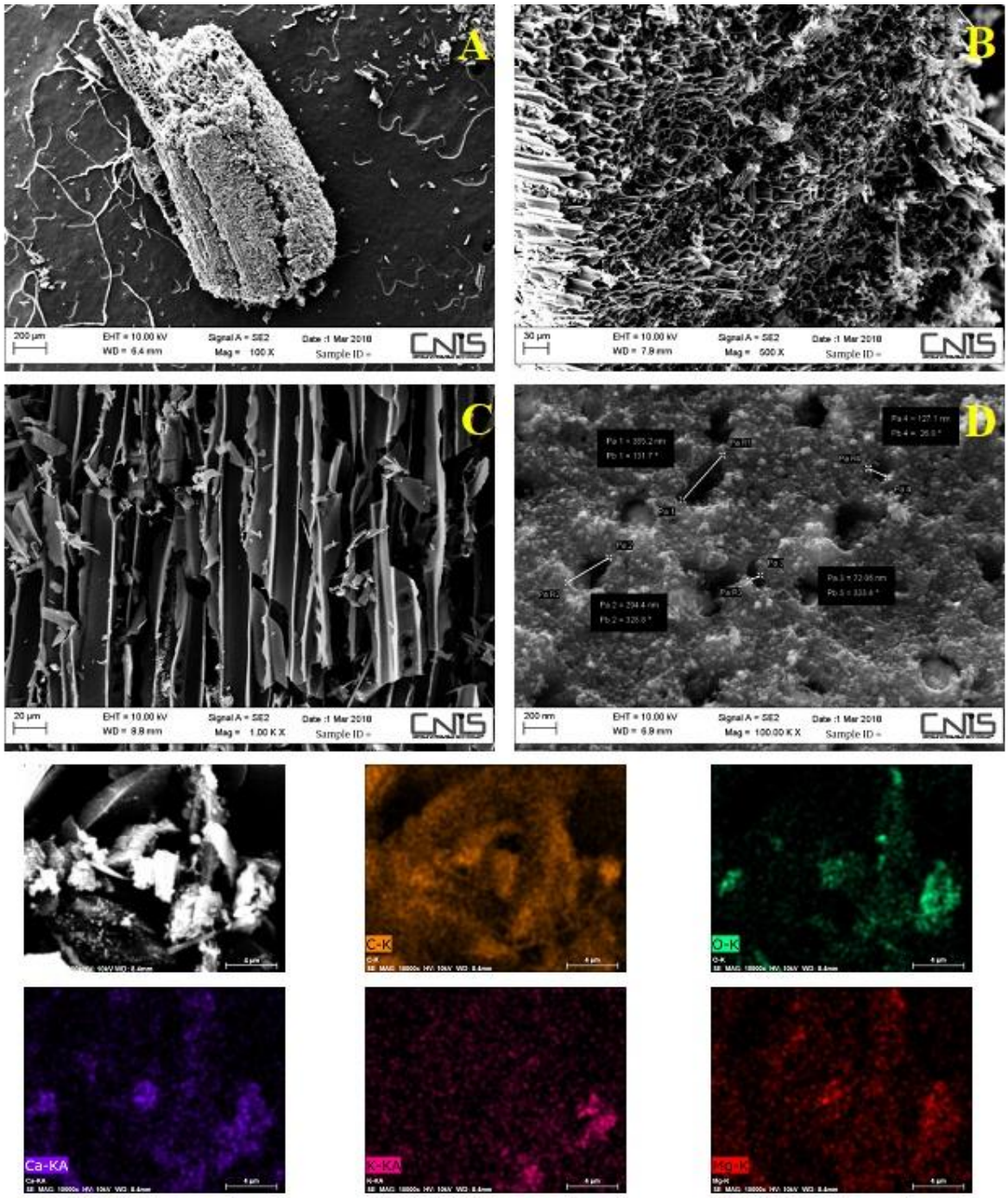

Figure 1. Scanning Electron Microscope (SEM) images of the surface and image and color coded Energy Dispersive X-ray (EDX) analysis dot maps of RE-CHAR® at different magnifications: (A) 100 X; (B) 500 X; (C) 1.00 KX; and (D) 100.00 KX.

Figure 1 (A) highlights one chip of biochar, (B) is the transversal cut cross-section, (C) the longitudinal vertically cut cross-section and (D) variously sized pores.

From the graphic extrapolations in Figure 1, the average dimension of pores in relation to the magnification used was obtained during image acquisition, i.e. 210 ± 4.0 nm at 100.00 KX.

Figure 1 shows also the elemental maps of carbon, oxygen, calcium, potassium and magnesium within the biochar samples, whose percentage contents are reported in Table 2. Particularly, amber color is used to indicate carbon, aquamarine for oxygen, dark violet for calcium, magenta for potassium and red for magnesium.

3.2. Batch tests

Figure 2 shows lead percentage removal versus time measured in the batch tests conducted at initial concentrations of 50 mg/L and 100 mg/L Pb. It can be observed that removal rate was initially very fast, reaching values of 70% at 50 mg/L and 85% at 100 mg/L after only 30 min. Thereafter, in the case of C_0 = 100 mg/L, it proceeded at a much lower rate, reaching R% = 100% after 4 h contact time. For C_0 = 50 mg/L, the removal remained constant at about 70% until the end of the first hour (t = 1 h) and then increased rapidly assuming a profile similar to that observed at C_0 = 100 mg/L; a complete removal (R% = 100%) was reached at the same time, i.e. t = 4 h. Negligible variations were observed afterwards.

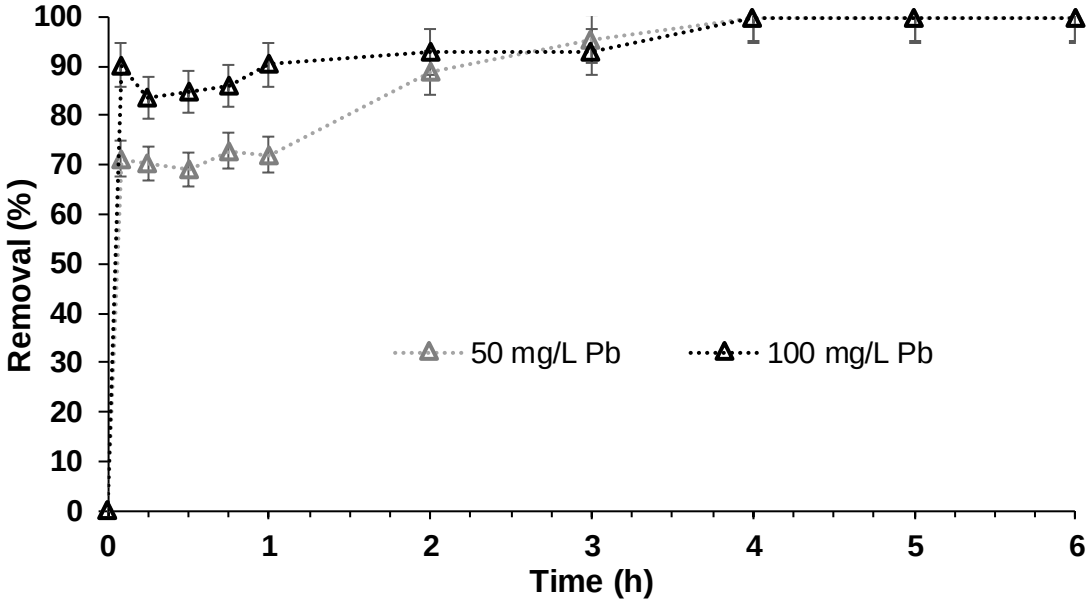

Figure 2. Lead percentage removal versus contact time. Adsorption temperature, mixing rate and biochar dosage: 20 ± 0.5 °C, 120 rpm, 5 g/L.

These results are consistent with the scientific literature: for instance, in Kołodyńska et al. (2012), a similar time-profile was reported for Pb adsorption at the same initial concentration onto biochar produced from pyrolysis of pig and cow manure at 400 °C and 600 °C, although at a slower rate (equilibria was reached after 5 h contact time). Lead sorption, with initial concentrations ranging from 5 to 200 ppm, onto biochar from pyrolysis of raw sugarcane bagasse also reached equilibrium after about 5 h (M. Inyang et al. 2011). The same equilibrium time (5 h) was found in a previous paper by the same authors (Boni et al. 2018b), where the tested biochar was produced by pyrolysis of poplar, oak, robinia, platanus, willow, apple and pear wood. Another study indicated equilibrium times after about 2 hour for the adsorption of 50 mg/L Pb onto a biochar made from a mixture of wood chips, green waste, rice hull, corn cob, nut shells and husks, and cotton gin trash and pomace (Karunanayake et al. 2018). In the same paper (Karunanayake et al. 2018), adsorption on biochar of pinewood and of magnetic switch-grass, at the same Pb concentration, required from 8 to 20 h to reach equilibrium.

Therefore, considering the results obtained in the present study and those reported by the literature, it is evident that feedstock and operating conditions of the production process of RE-CHAR® influence the rate of removal.

The linearized form of the equation of the different kinetic models was used to find out the best fitting of the experimental data. The pseudo second-order model provided the best agreement for both Pb concentrations (higher R^2 value) with respect to the other applied models. Figure 3 shows the experimental and the modelled data in terms of t/q_t versus t. The pseudo second-order equation assumes that the rate of occupation of adsorption sites is proportional to the square of the number of unoccupied activated sites on the surface of the adsorbent (Ho and McKay 1999).

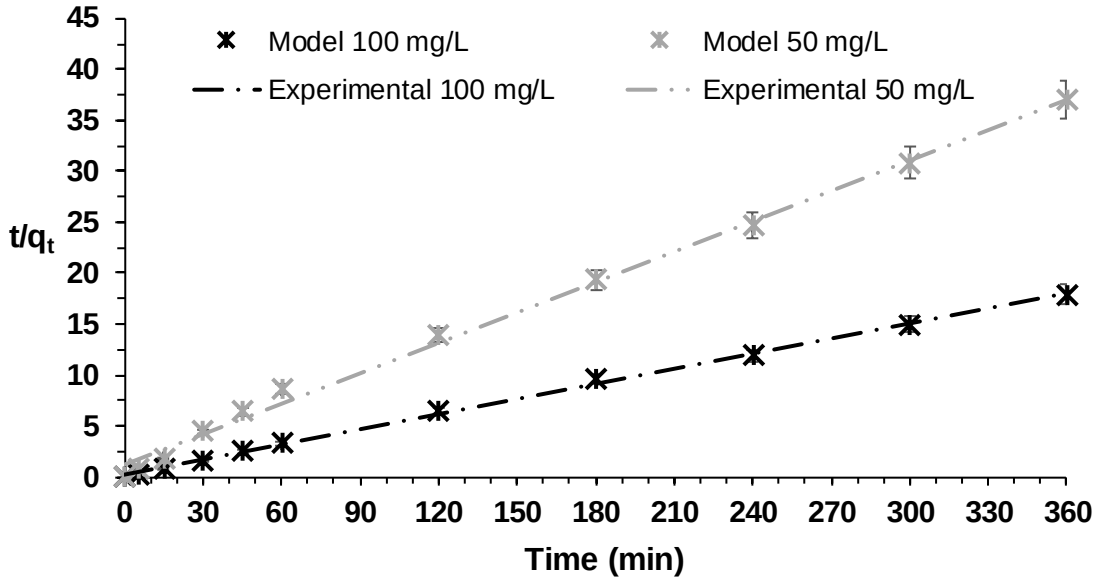

Figure 3. Kinetic experimental data and modelled by the linearized pseudo-second-order equation. Adsorption temperature, mixing rate and biochar dosage: 20 ± 0.5 °C, 120 rpm, 5 g/L.

Through the slope and intercept of the regression line, it was possible to determine the values of the pseudo second-order rate constant, k_s, and of the amount of Pb adsorbed at

equilibrium per unit weight of RE-CHAR®, q_e, both reported in Table 3. The same table also shows $q_{e,exp}$ which represents the value of q experimentally calculated at t = 300 min, which was assumed to be the equilibrium time based on the batch tests results. It can be noted that experimental and modelled data of the adsorption capacity do not differ appreciably in both cases of 50 mg/L and 100 mg/L Pb.

Table 3. Pseudo second-order kinetic model parameters.

C_0 (mg/L)	$q_{e,exp}$ (mg/g)	q_e (mg/g)	k_s (g/min)	R^2 -
50	9.7340	9.9957	0.0091	0.9959
100	20.0800	20.1462	0.0128	0.9988

Comparing the values obtained for the specific adsorption capacity, it can be noted an almost linear increase of q_e with concentration: for instance, rising Pb in solution from 50 mg/L to 100 mg/L led to a double q_e value.

Other studies found that the pseudo second order model was that one better representing the biochar adsorption process of lead at the same initial concentration as in the present paper (Boni et al. 2018b; Deng et al. 2017; H. Lu et al. 2012) or at a double concentration (Ifthikar et al. 2017).

The Langmuir model (Langmuir 1918) provided the best agreement (higher R^2 value) of the experimental data obtained in the equilibrium tests, with respect to Freundlich (1907) and BET (1938) isotherms, for the lead contaminated water at 50 mg/L Pb (R^2 = 0.5918 and R^2 = 0.9809, respectively) and 100 mg/L Pb (R^2 = 0.5398 and R^2 = 0.9860, respectively).

Langmuir model assumes a monolayer adsorption of solutes onto a surface comprised of a finite number of identical sites with homogeneous adsorption energy (Sivaraj et al. 2001).

This means that once a molecule occupies a binding site, no further adsorption can take place at that site (Ali et al. 2016). The essential characteristics of Langmuir isotherm can be expressed in terms of the dimensionless constant separation factor (R_L) for the equilibrium conditions (Langmuir 1918; T. W. Weber and Chakravorti 1974). This parameter is defined as:

$$R_L = \frac{1}{(1 + bC_0)} \quad (4)$$

where C_0 is the Pb initial concentration (mg/L) and b is the Langmuir constant (L/mg). According to Hall et al. (1966), using mathematical calculations, it has been shown that the parameter R_L indicates the isotherm to be irreversible ($R_L = 0$), favourable ($0 < R_L < 1$), linear ($R_L = 1$) or unfavourable ($R_L > 1$).

Plotting C_e/q_e versus C_e follows approximately a straight line, as highlighted in Figure 4.

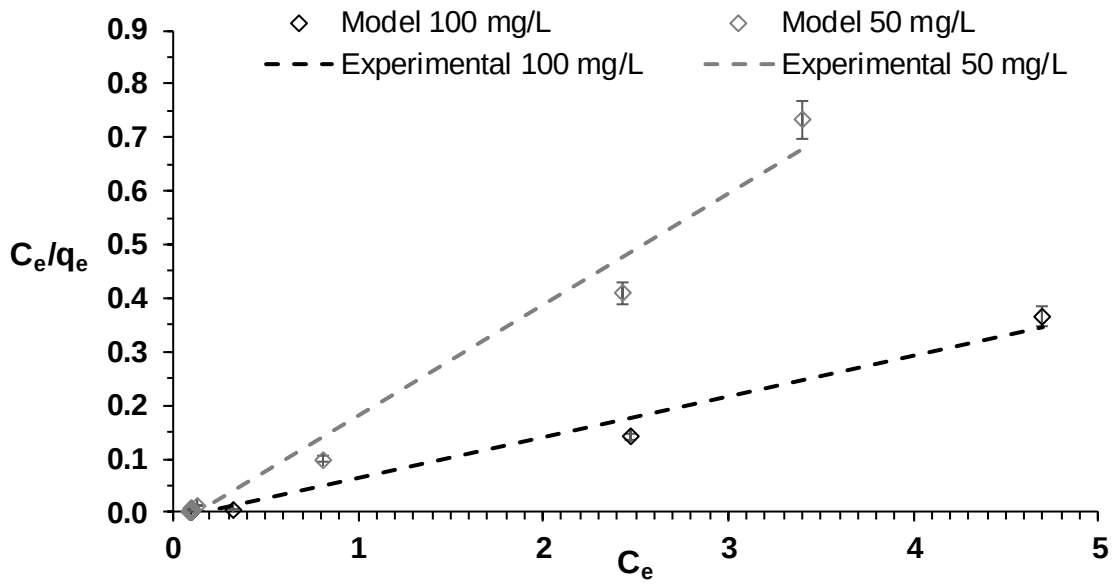

Figure 4. Equilibrium experimental and modelled data by the linearized Langmuir equation. Adsorption temperature, mixing rate and equilibrium time: 20 ± 0.5 °C, 120 rpm, 5 h.

From the slope and intercept of the regression line, it was possible to calculate the values of the maximum adsorption capacity, q_{max}, and the constant b, which are reported in Table 4.Specifically, q_{max} represents the amount of solute adsorbed per unit mass of adsorbent which is required for the monolayer coverage of the surface (mg/g), also called monolayer capacity; b is the Langmuir constant related to the affinity between the sorbent and sorbate (L/mg).

Table 4. Adsorption Langmuir isotherm parameters.

C_0	q_{max}	b	R^2	R_L
(mg/L)	(mg/g)	(L/mg)	-	-
50	4.6116	11.5804	0.9967	0.0017
100	9.5895	2.8933	0.9863	0.0032

Values of R_L were found to be slightly above zero for both lead concentrations (i.e. R_L = 0.0017 and R_L = 0.0032 for 50 mg/L Pb and 100 mg/L Pb, respectively), thus indicating that the adsorption process of Pb was always slightly favourable.

In terms of implementation at full-scale, adsorbents with the highest value of the maximum adsorption capacity, q_{max}, are the most desirable. The values found in the present study for RE-CHAR® fall within the ranges referred by the literature for different biochars used for Pb removal from water solutions (Harris 2009; M. Inyang et al. 2011; M. I. Inyang et al. 2016; Y.-H. Li et al. 2003; Liu and Zhang 2009; Mahdi et al. 2018; Mohan et al. 2007, 2014; Uchimiya et al. 2010). For instance, Liu and Zhang (2009), by applying biochar

prepared from hydrothermal liquefaction of pinewood (P300) to a Pb solution of about 50 mg/L, found for the maximum lead sorption capacity a very similar value to that obtained in the present study (i.e. 4.25 mg/g, and 4.61 mg/g, respectively).

Using biochar produced at 500° C from sugarcane bagasse and Pb concentration of about 80 mg/L, the adsorption capacity resulted to be. 9.13 mg/g, which does not differ appreciably from 9.58 mg/g observed in the present study at 100 mg/L (W. Ding et al. 2014).

The slight differences are likely due to the change in the type and operating conditions of the production process, which are known to affect the porosity and microstructure of the adsorbents (W. Ding et al. 2014; Liu and Zhang 2009); these in turn influence the amount of pollutant that can be adsorbed per unit weight of media.

The ability of RE-CHAR® to remove lead as a function of the adsorbent mass is shown in Figure 5.

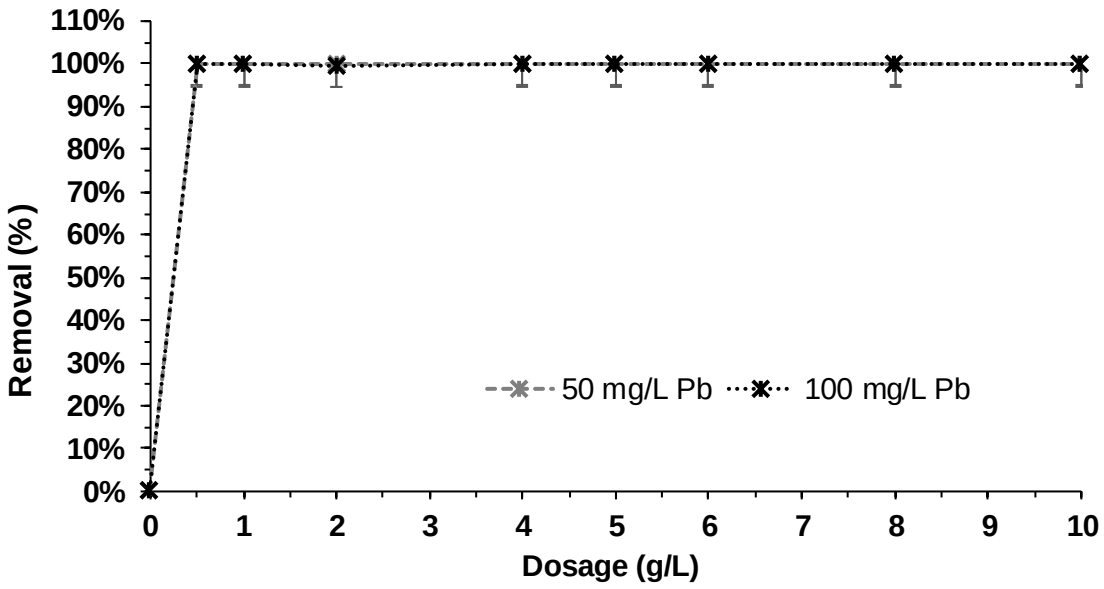

Figure 5. Percentage of lead removal versus different RE-CHAR® dosages at 50 mg/L and 100 mg/L Pb. Adsorption temperature, mixing rate and equilibrium time: 20 ± 0.5 °C, 120 rpm, 5 h.

It is highlighted that a dosage of 0.5 g/L RE-CHAR® was the minimum required to achieve the highest removal percentage, i.e. R% = 100%, at both concentrations of 50 mg/L and 100 mg/L Pb.

From this figure it can be deemed that, for Pb contaminated solutions at 50 mg/L and 100 mg/L, using a dosage of 1 g/L of RE-CHAR® adsorbent makes it possible to comply with the limit set by the Italian legislation for discharge into surface waters and sewage systems (respectively 0.2 mg/L and 0.3 mg/L).

3.3. Column tests

Figure 6 shows the breakthrough curves obtained through the column tests. The curves represent the percentage ratio of Pb concentration in the eluate and in the feeding solution, i.e. C/C_0, versus time of operation of the column plant filled with soil only and soil and RE-CHAR®. Figure 6 also shows two horizontal lines drawn at C/C_0 = 5% and C/C_0 = 95%, assumed to represent the breakthrough and exhaustion conditions, respectively.

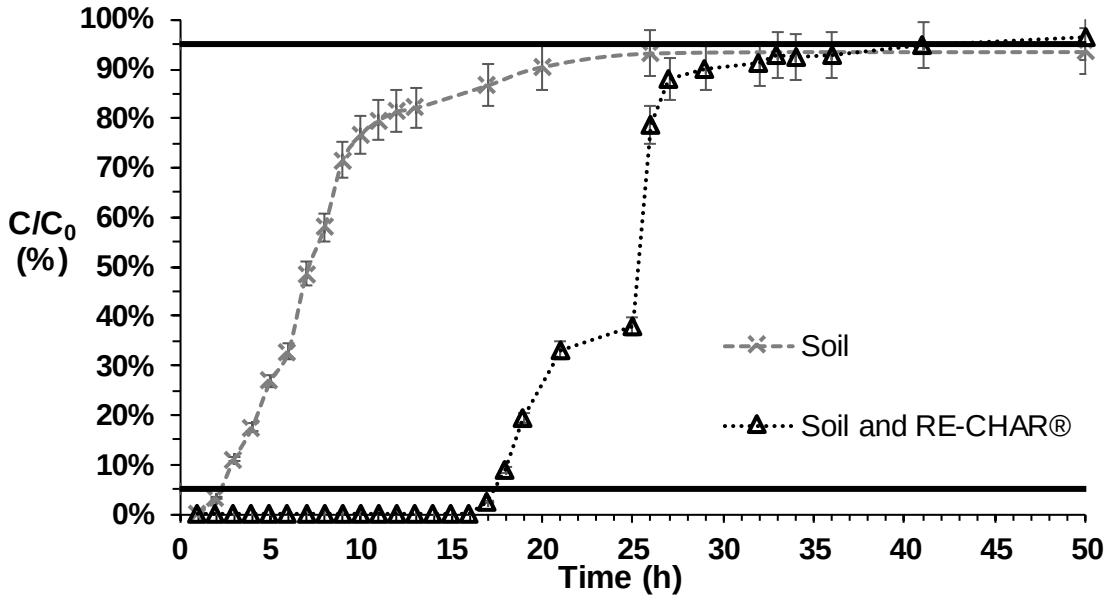

Figure 6. Breakthrough curves for adsorption of Pb onto soil and soil and RE-CHAR® in the column plants. Adsorption temperature, flow rate and initial Pb concentration: 20 ± 0.5 °C, 60 mL/h, 100 mg/L.

The breakthrough curves obtained for soil and soil and biochar columns showed approximately the same shape: a rapid increase of C/C_0 after breakthrough (C/C_0 = 5%), followed by a trend at a much slower rate towards the exhaustion (C/C_0 = 95%). However, it is worth noting that breakthrough times were reached much faster in the column containing soil only with respect to the column filled with soil and biochar: i.e. few hours and 15 h, respectively. Similarly, exhaustion times appeared after about 25 h and 40 h, respectively.

The breakthrough curves of Pb adsorption onto soil and soil and RE-CHAR®, reported in Figure 6, highlight that the addition of biochar significantly enhanced the adsorption capacity and the operation time of the column plant with respect to the column containing only soil. This implies a higher amount of metal uptaken by the adsorbent and a less frequency of adsorbent bed replacement/regeneration after exhaustion, which lead to reduced operating costs of the treatment plant.

Within the specialized literature only one reference could be found on the application of biochar as adsorbent media in a column plant for lead removal from water, which is the work by the same authors (Boni et al. 2018b). Therefore, the findings of the present study can play a key role in view of the implementation of this adsorption process at full-scale which usually applies a column system.

By integrating the breakthrough curves between t = 0 and t = 50 h (which was fixed as the end of the column tests), it was possible to determine the experimental value of the adsorption capacity: this resulted to be equal to q_{exp} = 230.96 mg/g for the column filled with soil and RE-CHAR® and q_{exp} = 67.07 mg/g for the column containing soil only. Taking into

account that the amount of soil was the same in both columns, the adsorption capacity of RE-CHAR® only it was calculated to be 163.89 mg/g.

Among the three mathematical models tested, the Thomas equation provided a better description of the experimental breakthrough curves (R^2 = 0.853), compared to Yoon–Nelson (R^2 = 0.850) and Bohart–Adams (R^2 = 0.788). Boni et al. (2018b) also found that Thomas model provided the best fitting of the breakthrough curve experimental data, using biochar from poplar, oak, robinia, platanus, willow, apple and pear wood, for the treatment of a lead contaminated solution. The Thomas rate constant (k_{TH}) and the adsorption capacity (q_0) were obtained from the intercept and the slope of the linearized form of the model equation. By plotting $\ln(C_0/C\text{-}1)$ versus t, the following values were found: $k_{TH} = 5.28 \times 10^{-5}$ mL/min·mg and q_0 = 334.57 mg/g.

The adsorption capacity predicted by the model was higher than that experimentally determined, i.e. q_{exp} = 230.96 mg/g: the difference indicates that the adsorbent media had not reached complete saturation at the end of the tests, i.e. at t = 50 h, and therefore it still possessed adsorption sites which could be potentially occupied by the adsorbate. As expected, the higher driving force of the adsorption process acting in the continuous flow column plant determined a higher uptake capacity than that measured under batch conditions.

In the paper above cited (Boni et al. 2018b), the adsorption capacity predicted by the Thomas model was found to be of the same order of magnitude. thus confirming the data herewith obtained; however, the previous study measured a value of q_0 = 270.57 mg/g which is slightly lower, likely due to the different type of feed source for the biochar.

The value of q_0 predicted by the model was very similar to the data reported in the specialized literature for the lead maximum adsorption capacity by adsorbents other than biochar used in column plants (Boni et al. 2018b; Harris 2009; M. Inyang et al. 2011; M. I.

Inyang et al. 2016; Y.-H. Li et al. 2003; Liu and Zhang 2009; Mahdi et al. 2018; Mohan et al. 2007; Uchimiya et al. 2010).

4. Conclusions

The present paper demonstrated that RE-CHAR® biochar, which is currently used as a soil improver, can be also considered an efficient adsorbent media for the remediation of highly lead-contaminated solutions.

For instance, in batch applications, a low dosage and a short contact time are needed to treat the contaminated solution to the point that it is possible to release it into surface waters and sewage systems complying with the limits set by the Italian legislation

In the continuous flow applications, operation times of the column plants can be significantly extended by adding biochar to the soil within the adsorbent bed.

Therefore, application of RE-CHAR® biochar in place of commercial adsorbents is technically and economically feasible.

For the optimal exploitation of the RE-CHAR® biochar capacity, further tests are required under real operating conditions and with more complex contaminated solutions.

Acknowledgments

The authors wish to thank RECORD IMMOBILIARE S.r.l. who provided RE-CHAR® biochar.

References

Abadin, H., Ashizawa, A., Stevens, Y.-W., Llados, F., Diamond, G., Sage, G., et al. (2007). Toxicological Profile for Lead. *U.S Public Health Service, Agency for Toxic Substances*

481 *and Disease Registry*, (August), 582.
482 Agegnehu, G., Srivastava, A. K., & Bird, M. I. (2017). The role of biochar and biochar-
483 compost in improving soil quality and crop performance: A review. *Applied Soil*
484 *Ecology*, *119*(April), 156–170. https://doi.org/10.1016/j.apsoil.2017.06.008
485 Ahmad, M., Rajapaksha, A. U., Lim, J. E., Zhang, M., Bolan, N., Mohan, D., et al. (2014).
486 Biochar as a sorbent for contaminant management in soil and water: A review.
487 *Chemosphere*, *99*, 19–23. https://doi.org/10.1016/j.chemosphere.2013.10.071
488 Ahmed, M. B., Zhou, J. L., Ngo, H. H., & Guo, W. (2016a). Insight into biochar properties
489 and its cost analysis. *Biomass and Bioenergy*, *84*, 76–86.
490 https://doi.org/10.1016/j.biombioe.2015.11.002
491 Ahmed, M. B., Zhou, J. L., Ngo, H. H., Guo, W., & Chen, M. (2016b). Progress in the
492 preparation and application of modified biochar for improved contaminant removal from
493 water and wastewater. *Bioresource Technology*, *214*, 836–851.
494 https://doi.org/10.1016/j.biortech.2016.05.057
495 Ali, R. M., Hamad, H. A., Hussein, M. M., & Malash, G. F. (2016). Potential of using green
496 adsorbent of heavy metal removal from aqueous solutions: Adsorption kinetics, isotherm,
497 thermodynamic, mechanism and economic analysis. *Ecological Engineering*, *91*, 317–
498 332. https://doi.org/10.1016/j.ecoleng.2016.03.015
499 Allaire, S. E., Lange, S. F., Auclair, I. K., Quinche, M., & Greffard, L. (2015). *Analyses of*
500 *biochar properties*. *CRMR-2015-SA-5*. Québec, QC, Canada.
501 https://doi.org/10.13140/rg.2.1.2789.4241
502 Aller, M. F. (2016). Biochar properties: Transport, fate, and impact. *Critical Reviews in*
503 *Environmental Science and Technology*, *46*(14–15), 1183–1296.
504 https://doi.org/10.1080/10643389.2016.1212368
505 APAT, & IRSA/CNR. (2003). *Metodi analitici per le acque*. (M. Belli, D. Centioli, P. De

Zorzi, U. Sansone, S. Capri, R. Pagnotta, & M. Pettine, Eds.). Rome, Italy: APAT. http://www.isprambiente.gov.it/it/pubblicazioni/manuali-e-linee-guida/metodi-analitici-per-le-acque

Bashir, S., Hussain, Q., Akmal, M., Riaz, M., Hu, H., Ijaz, S. S., et al. (2018). Sugarcane bagasse-derived biochar reduces the cadmium and chromium bioavailability to mash bean and enhances the microbial activity in contaminated soil. *Journal of Soils and Sediments*, *18*(3), 874–886. https://doi.org/10.1007/s11368-017-1796-z

Basu, P. (2010). *Biomass Gasification and Pyrolysis: Pratical Design and Theory*. (Elsevier, Ed.). https://doi.org/10.1016/C2009-0-20099-7

Beesley, L., Inneh, O. S., Norton, G. J., Moreno-Jimenez, E., Pardo, T., Clemente, R., & Dawson, J. J. C. (2014). Assessing the influence of compost and biochar amendments on the mobility and toxicity of metals and arsenic in a naturally contaminated mine soil. *Environmental Pollution*, *186*, 195–202. https://doi.org/10.1016/j.envpol.2013.11.026

Beesley, L., Moreno-Jiménez, E., Gomez-Eyles, J. L., Harris, E., Robinson, B., & Sizmur, T. (2011). A review of biochars' potential role in the remediation, revegetation and restoration of contaminated soils. *Environmental Pollution*, *159*(12), 3269–3282. https://doi.org/10.1016/j.envpol.2011.07.023

Bhaumik, M., Setshedi, K., Maity, A., & Onyango, M. S. (2013). Chromium(VI) removal from water using fixed bed column of polypyrrole/Fe3O4 nanocomposite. *Separation and Purification Technology*, *110*, 11–19. https://doi.org/10.1016/j.seppur.2013.02.037

Blanco-Canqui, H. (2017). Biochar and Soil Physical Properties. *Soil Science Society of America Journal*, *84*(4), 687–711. https://doi.org/10.2136/sssaj2017.01.0017

Bohart, G. S., & Adams, E. Q. (1920). Some aspects of the behavior of charcoal with respect to chlorine. *Journal of the American Chemical Society*, *42*(3), 523–544. https://doi.org/10.1021/ja01448a018

Boni, M. R., Chiavola, A., Antonucci, A., Di Mattia, E., & Marzeddu, S. (2018a). A novel treatment for Cd-contaminated solution through adsorption on beech charcoal: the effect of bioactivation. *Desalination and Water Treatment*, *127*, 104–110. https://doi.org/10.5004/dwt.2018.22664

Boni, M. R., Chiavola, A., & Marzeddu, S. (2018b). Application of Biochar to the Remediation of Pb-Contaminated Solutions. *Sustainability*, *10*(12), 4440. https://doi.org/10.3390/su10124440

Brunauer, S., Emmett, P. H., & Teller, E. (1938). Adsorption of gases in multimolecular layers. *Journal of the American Chemical Society*, *60*(2), 309–319. https://doi.org/10.1021/ja01269a023

Burrell, L. D., Zehetner, F., Rampazzo, N., Wimmer, B., & Soja, G. (2016). Long-term effects of biochar on soil physical properties. *Geoderma*, *282*, 96–102. https://doi.org/10.1016/j.geoderma.2016.07.019

Cha, J. S., Park, S. H., Jung, S. C., Ryu, C., Jeon, J. K., Shin, M. C., & Park, Y. K. (2016). Production and utilization of biochar: A review. *Journal of Industrial and Engineering Chemistry*, *40*, 1–15. https://doi.org/10.1016/j.jiec.2016.06.002

Chen, B., Zhou, D., & Zhu, L. (2008). Transitional adsorption and partition of nonpolar and polar aromatic contaminants by biochars of pine needles with different pyrolytic temperatures. *Environmental Science and Technology*, *42*(14), 5137–5143. https://doi.org/10.1021/es8002684

Chern, J. M., & Chien, Y. W. (2002). Adsorption of nitrophenol onto activated carbon: Isotherms and breakthrough curves. *Water Research*, *36*(3), 647–655. https://doi.org/10.1016/S0043-1354(01)00258-5

Chiavola, A., D'Amato, E., Stoller, M., Chianese, A., & Boni, M. R. (2016). Application of iron based nanoparticles as adsorbents for Arsenic removal from water. *Chemical*

Engineering Transactions, *47*, 325–330. https://doi.org/10.3303/CET1647055

Cobbina, S. J., Nkuah, D., Tom-Dery, D., & Obiri, S. (2013). Non-cancer risk assessment from exposure to mercury (Hg), cadmium (Cd), arsenic (As), copper (Cu) and lead (Pb) in boreholes and surface water in Tinga, in the Bole-Bamboi District, Ghana. *Journal of Toxicology and Environmental Health Sciences*, *5*(2), 29–36. https://doi.org/10.5897/jtehs12.0253

De Gisi, S., Lofrano, G., Grassi, M., & Notarnicola, M. (2016). Characteristics and adsorption capacities of low-cost sorbents for wastewater treatment: A review. *Sustainable Materials and Technologies*, *9*, 10–40. https://doi.org/10.1016/j.susmat.2016.06.002

Deng, J., Liu, Y., Liu, S., Zeng, G., Tan, X., Huang, B., et al. (2017). Competitive adsorption of Pb(II), Cd(II) and Cu(II) onto chitosan-pyromellitic dianhydride modified biochar. *Journal of Colloid and Interface Science*, *506*, 355–364. https://doi.org/10.1016/j.jcis.2017.07.069

Ding, W., Dong, X., Ime, I. M., Gao, B., & Ma, L. Q. (2014). Pyrolytic temperatures impact lead sorption mechanisms by bagasse biochars. *Chemosphere*, *105*, 68–74. https://doi.org/10.1016/j.chemosphere.2013.12.042

Ding, Z., Hu, X., Wan, Y., Wang, S., & Gao, B. (2016). Removal of lead, copper, cadmium, zinc, and nickel from aqueous solutions by alkali-modified biochar: Batch and column tests. *Journal of Industrial and Engineering Chemistry*, *33*, 239–245. https://doi.org/10.1016/j.jiec.2015.10.007

Febrianto, J., Kosasih, A. N., Sunarso, J., Ju, Y. H., Indraswati, N., & Ismadji, S. (2009). Equilibrium and kinetic studies in adsorption of heavy metals using biosorbent: A summary of recent studies. *Journal of Hazardous Materials*, *162*(2–3), 616–645. https://doi.org/10.1016/j.jhazmat.2008.06.042

Flora, G., Gupta, D., & Tiwari, A. (2012). Toxicity of lead: A review with recent updates.

Interdisciplinary Toxicology, *5*(2), 47–58. https://doi.org/10.2478/v10102-012-0009-2

Freundlich, H. M. F. (1907). Über die Adsorption in Lösungen. *Zeitschrift für Physikalische Chemie*, *57*(1), 385–470. https://doi.org/10.1515/zpch-1907-5723

Glaser, B. (2007). Prehistorically modified soils of central Amazonia: a model for sustainable agriculture in the twenty-first century. *Philosophical Transactions of the Royal Society B: Biological Sciences*, *362*(1478), 187–196. https://doi.org/10.1098/rstb.2006.1978

Glaser, B., Lehmann, J., & Zech, W. (2002). Ameliorating physical and chemical properties of highly weathered soils in the tropics with charcoal - A review. *Biology and Fertility of Soils*, *35*(4), 219–230. https://doi.org/10.1007/s00374-002-0466-4

Hagemann, N., Joseph, S., Schmidt, H. P., Kammann, C. I., Harter, J., Borch, T., et al. (2017). Organic coating on biochar explains its nutrient retention and stimulation of soil fertility. *Nature Communications*, *8*(1), 1–11. https://doi.org/10.1038/s41467-017-01123-0

Hagemann, N., Spokas, K., Schmidt, H. P., Kägi, R., Böhler, M. A., & Bucheli, T. D. (2018). Activated carbon, biochar and charcoal: Linkages and synergies across pyrogenic carbon's ABCs. *Water (Switzerland)*, *10*(182), 1–19. https://doi.org/10.3390/w10020182

Hai, F. I., Yamamoto, K., & Jegatheesan, J. V. (2018). *Wastewater Treatment and Reuse Technologies*. (F. I. Hai, K. Yamamoto, & J. V. Jegatheesan, Eds.)*Printed edition of the Special Issue Wastewater Treatment and Reuse Technologies* (1st ed.). MDPI. https://doi.org/10.3390/books978-3-03897-102-3

Hall, K. R., Eagleton, L. C., Acrivos, A., & Vermeulen, T. (1966). Pore- and solid-diffusion kinetics in fixed-bed adsorption under constant-pattern conditions. *Industrial and Engineering Chemistry Fundamentals*, *5*(2), 212–223. https://doi.org/10.1021/i160018a011

Hanna-Attisha, M., LaChance, J., Sadler, R. C., & Schnepp, A. C. (2016). Elevated blood lead levels in children associated with the flint drinking water crisis: A spatial analysis of risk

606 and public health response. *American Journal of Public Health*, *106*(2), 283–290.
607 https://doi.org/10.2105/AJPH.2015.303003
608 Harris, W. (2009). Dairy-Manure Derived Biochar Effectively Sorbs Lead and Atrazine.
609 *Environmental Science and Technology*, *1*(352), 3285–3291. https://doi.org/Doi
610 10.1021/Es803092k
611 Ho, Y. S., & McKay, G. (1999). Pseudo-second order model for sorption processes. *Process*
612 *Biochemistry*, *34*(5), 451–465. https://doi.org/10.1016/S0032-9592(98)00112-5
613 Ifthikar, J., Wang, T., Khan, A., Jawad, A., Sun, T., Jiao, X., et al. (2017). Highly Efficient
614 Lead Distribution by Magnetic Sewage Sludge Biochar: Sorption Mechanisms and
615 Bench Applications. *Bioresource Technology*, *238*, 399–406.
616 https://doi.org/10.1016/j.biortech.2017.03.133
617 Inyang, M., Gao, B., Ding, W., Pullammanappallil, P., Zimmerman, A. R., & Cao, X. (2011).
618 Enhanced lead sorption by biochar derived from anaerobically digested sugarcane
619 bagasse. *Separation Science and Technology*, *46*(12), 1950–1956.
620 https://doi.org/10.1080/01496395.2011.584604
621 Inyang, M. I., Gao, B., Yao, Y., Xue, Y., Zimmerman, A., Mosa, A., et al. (2016). A review of
622 biochar as a low-cost adsorbent for aqueous heavy metal removal. *Critical Reviews in*
623 *Environmental Science and Technology*, *46*(4), 406–433.
624 https://doi.org/10.1080/10643389.2015.1096880
625 Janus, A., Pelfrêne, A., Heymans, S., Deboffe, C., Douay, F., & Waterlot, C. (2015).
626 Elaboration, characteristics and advantages of biochars for the management of
627 contaminated soils with a specific overview on Miscanthus biochars. *Journal of*
628 *Environmental Management*, *162*, 275–289.
629 https://doi.org/10.1016/j.jenvman.2015.07.056
630 Jien, S. H., Chen, W. C., Ok, Y. S., Awad, Y. M., & Liao, C. Sen. (2017). Short-term biochar

631 application induced variations in C and N mineralization in a compost-amended tropical
632 soil. *Environmental Science and Pollution Research*, 1–11.
633 https://doi.org/10.1007/s11356-017-9234-8
634 Jindo, K., Mizumoto, H., Sawada, Y., Sanchez-Monedero, M. A., & Sonoki, T. (2014).
635 Physical and chemical characterization of biochars derived from different agricultural
636 residues. *Biogeosciences*, *11*(23), 6613–6621. https://doi.org/10.5194/bg-11-6613-2014
637 Joseph, S., Xu, C. Y., Wallace, H. M., Farrar, M., Nhan Nguyen, T. T., Bai, S. H., &
638 Solaiman, Z. M. (2017). Biochar Production From Agricultural and Forestry Wastes and
639 Microbial Interactions. In *Current Developments in Biotechnology and Bioengineering:*
640 *Solid Waste Management* (pp. 443–473). Elsevier. https://doi.org/10.1016/B978-0-444-
641 63664-5.00019-8
642 Kan, T., Strezov, V., & Evans, T. J. (2016). Lignocellulosic biomass pyrolysis: A review of
643 product properties and effects of pyrolysis parameters. *Renewable and Sustainable*
644 *Energy Reviews*, *57*, 126–1140. https://doi.org/10.1016/j.rser.2015.12.185
645 Karunanayake, A. G., Todd, O. A., Crowley, M., Ricchetti, L., Pittman, C. U., Anderson, R.,
646 et al. (2018). Lead and cadmium remediation using magnetized and non magnetized
647 biochar from Douglas fir. *Chemical Engineering Journal*, *331*(June 2017), 480–491.
648 https://doi.org/10.1016/j.cej.2017.08.124
649 Kasozi, G. N., Zimmerman, A. R., Nkedi-Kizza, P., & Gao, B. (2010). Catechol and Humic
650 Acid Sorption onto a Range of Laboratory Produced Black Carbons (Biochars).
651 *Environmental Science and Technology*, *44*(16), 6189–6195.
652 https://doi.org/10.1021/es1014423
653 Keske, C., Godfrey, T., Hoag, D. L. K., & Abedin, J. (2019). Economic feasibility of biochar
654 and agriculture coproduction from Canadian black spruce forest. *Food and Energy*
655 *Security*, (October), 1–11. https://doi.org/10.1002/fes3.188

656 Klasson, K. T. (2017). Biochar characterization and a method for estimating biochar quality
657 from proximate analysis results. *Biomass and Bioenergy*, *96*, 50–58.
658 https://doi.org/10.1016/j.biombioe.2016.10.011
659 Kołodyńska, D., Krukowska, J., & Thomas, P. (2017). Comparison of sorption and desorption
660 studies of heavy metal ions from biochar and commercial active carbon. *Chemical*
661 *Engineering Journal*, *307*, 353–363. https://doi.org/10.1016/j.cej.2016.08.088
662 Kołodyńska, D., Wnetrzak, R., Leahy, J. J., Hayes, M. H. B., Kwapiński, W., & Hubicki, Z.
663 (2012). Kinetic and adsorptive characterization of biochar in metal ions removal.
664 *Chemical Engineering Journal*, *197*, 295–305. https://doi.org/10.1016/j.cej.2012.05.025
665 Kong, H., He, J., Gao, Y., Wu, H., & Zhu, X. (2011). Cosorption of phenanthrene and
666 mercury(II) from aqueous solution by soybean stalk-based biochar. *Journal of*
667 *Agricultural and Food Chemistry*, *59*(22), 12116–12123.
668 https://doi.org/10.1021/jf202924a
669 Lange, S. F., Allaire, S. E., Charles, A., Auclair, I. K., Bajzak, C. E., Turgeon, L., & St-
670 Gelais, A. (2018). *Physicochemical Properties of 43 Biochars*. *CRMR-2018-SA-2-EN*.
671 Quebec, Qc., Canada. https://doi.org/10.13140/RG.2.2.25450.41924
672 Langmuir, I. (1918). The adsorption of gases on plane surfaces of glass, mica and platinum.
673 *Journal of the American Chemical Society*, *40*(9), 1361–1403.
674 https://doi.org/10.1021/ja02242a004
675 Lehmann, J., Rillig, M. C., Thies, J., Masiello, C. A., Hockaday, W. C., & Crowley, D.
676 (2011). Biochar effects on soil biota - A review. *Soil Biology and Biochemistry*, *43*(9),
677 1812–1836. https://doi.org/10.1016/j.soilbio.2011.04.022
678 Li, J., Dai, J., Liu, G., Zhang, H., Gao, Z., Fu, J., et al. (2016). Biochar from microwave
679 pyrolysis of biomass: A review. *Biomass and Bioenergy*, *94*, 228–244.
680 https://doi.org/10.1016/j.biombioe.2016.09.010

Li, R., Wang, J. J., Gaston, L. A., Zhou, B., Li, M., Xiao, R., et al. (2017). An overview of carbothermal synthesis of metal–biochar composites for the removal of oxyanion contaminants from aqueous solution. *Carbon*, *129*(April), 674–687. https://doi.org/10.1016/j.carbon.2017.12.070

Li, Y.-H., Ding, J., Luan, Z., Di, Z., Zhu, Y., Xu, C., et al. (2003). Competitive adsorption of Pb2+, Cu2+ and Cd2+ ions from aqueous solutions by multiwalled carbon nanotubes. *Carbon*, *41*(14), 2787–2792. https://doi.org/10.1016/S0008-6223(03)00392-0

Liu, Z., & Zhang, F. S. (2009). Removal of lead from water using biochars prepared from hydrothermal liquefaction of biomass. *Journal of Hazardous Materials*, *167*(1–3), 933–939. https://doi.org/10.1016/j.jhazmat.2009.01.085

Lomaglio, T., Hattab-Hambli, N., Miard, F., Lebrun, M., Nandillon, R., Trupiano, D., et al. (2018). Cd, Pb, and Zn mobility and (bio)availability in contaminated soils from a former smelting site amended with biochar. *Environmental Science and Pollution Research*, *25*, 25744–25756. https://doi.org/10.1007/s11356-017-9521-4

Lu, H., Zhang, W., Yang, Y., Huang, X., Wang, S., & Qiu, R. (2012). Relative distribution of Pb2+ sorption mechanisms by sludge-derived biochar. *Water Research*, *46*(3), 854–862. https://doi.org/10.1016/j.watres.2011.11.058

Lu, K., Yang, X., Gielen, G., Bolan, N., Ok, Y. S., Niazi, N. K., et al. (2017). Effect of bamboo and rice straw biochars on the mobility and redistribution of heavy metals (Cd, Cu, Pb and Zn) in contaminated soil. *Journal of Environmental Management*, *186*, 285–292. https://doi.org/10.1016/j.jenvman.2016.05.068

Luciano, A., Viotti, P., & Papini, M. P. (2010). Laboratory investigation of DNAPL migration in porous media. *Journal of Hazardous Materials*, *176*(1–3), 1006–1017. https://doi.org/10.1016/j.jhazmat.2009.11.141

Lugato, E., Vaccari, F. P., Genesio, L., Baronti, S., Pozzi, A., Rack, M., et al. (2013). An

706 energy-biochar chain involving biomass gasification and rice cultivation in Northern
707 Italy. *GCB Bioenergy*, *5*(2), 192–201. https://doi.org/10.1111/gcbb.12028
708 Mahdi, Z., Yu, Q. J., & El Hanandeh, A. (2018). Removal of lead(II) from aqueous solution
709 using date seed-derived biochar: batch and column studies. *Applied Water Science*, *8*(6),
710 181. https://doi.org/10.1007/s13201-018-0829-0
711 Mašek, O., Brownsort, P., Sohi, S. P., Cross, A., & Crombie, K. (2012). The effect of
712 pyrolysis conditions on biochar stability as determined by three methods. *GCB*
713 *Bioenergy*, *5*(2), 122–131. https://doi.org/10.1111/gcbb.12030
714 Mohan, D., Pittman, C. U., Bricka, M., Smith, F., Yancey, B., Mohammad, J., et al. (2007).
715 Sorption of arsenic, cadmium, and lead by chars produced from fast pyrolysis of wood
716 and bark during bio-oil production. *Journal of Colloid and Interface Science*, *310*(1), 57–
717 73. https://doi.org/10.1016/j.jcis.2007.01.020
718 Mohan, D., Sarswat, A., Ok, Y. S., & Pittman, C. U. (2014). Organic and inorganic
719 contaminants removal from water with biochar, a renewable, low cost and sustainable
720 adsorbent - A critical review. *Bioresource Technology*, *160*, 191–202.
721 https://doi.org/10.1016/j.biortech.2014.01.120
722 Mukherjee, A., Zimmerman, A. R., & Harris, W. (2011). Surface chemistry variations among
723 a series of laboratory-produced biochars. *Geoderma*, *163*(3–4), 247–255.
724 https://doi.org/10.1016/j.geoderma.2011.04.021
725 Naga Babu, A., Krishna Mohan, G. V., Kalpana, K., & Ravindhranath, K. (2017). Removal of
726 lead from water using calcium alginate beads doped with hydrazine sulphate-Activated
727 red mud as adsorbent. *Journal of Analytical Methods in Chemistry*, *2017*.
728 https://doi.org/10.1155/2017/4650594
729 Neilson, J. W., Artiola, J. F., & Maier, R. M. (2003). Characterization of lead removal from
730 contaminated soils by nontoxic soil-washing agents. *Journal of Environmental Quality*,

731 *32*(3), 899–908. https://doi.org/10.2134/jeq2003.8990
732 Nguyen, B. T., Lehmann, J., Hockaday, W. C., Joseph, S., & Masiello, C. A. (2010).
733 Temperature sensitivity of black carbon decomposition and oxidation. *Environmental*
734 *Science and Technology*, *44*(9), 3324–3331. https://doi.org/10.1021/es903016y
735 Nguyen, B. T., Lehmann, J., Kinyangi, J., Smernik, R., Riha, S. J., & Engelhard, M. H.
736 (2009). Long-term black carbon dynamics in cultivated soil. *Biogeochemistry*, *92*(1–2),
737 163–176. https://doi.org/10.1007/s10533-008-9248-x
738 Noh, J. S., & Schwarz, J. A. (1990). Effect of HNO3 treatment on the surface acidity of
739 activated carbons. *Carbon*, *28*(5), 675–682. https://doi.org/10.1016/0008-
740 6223(90)90069-B
741 Novak, J. M., Busscher, W. J., Laird, D. L., Ahmedna, M., Watts, D. W., & Niandou, M. A. S.
742 (2009). Impact of Biochar Amendment on Fertility of a Southeastern Coastal Plain Soil.
743 *Soil Science*, *174*(2), 105–112. https://doi.org/10.1097/ss.0b013e3181981d9a
744 Oliveira, F. R., Patel, A. K., Jaisi, D. P., Adhikari, S., Lu, H., & Khanal, S. K. (2017).
745 Environmental application of biochar: Current status and perspectives. *Bioresource*
746 *Technology*, *246*(July), 110–122. https://doi.org/10.1016/j.biortech.2017.08.122
747 Park, J. H., Lamb, D., Paneerselvam, P., Choppala, G., Bolan, N., & Chung, J. W. (2011).
748 Role of organic amendments on enhanced bioremediation of heavy metal(loid)
749 contaminated soils. *Journal of Hazardous Materials*, *185*(2–3), 549–574.
750 https://doi.org/10.1016/j.jhazmat.2010.09.082
751 Perry, R. H., & Green, D. W. (2008). *Perry's chemical engineers' handbook* (8°th Ed.).
752 McGraw-Hill: New York, Chicago, San Francisco, Lisbon, London, Madrid, Mexico
753 City, Milan, New Delhi, San Juan, Seoul, Singapore, Sydney, Toronto.
754 https://www.accessengineeringlibrary.com/browse/perrys-chemical-engineers-handbook-
755 eighth-edition. Accessed 9 October 2018

Pituello, C., Francioso, O., Simonetti, G., Pisi, A., Torreggiani, A., Berti, A., & Morari, F. (2015). Characterization of chemical–physical, structural and morphological properties of biochars from biowastes produced at different temperatures. *Journal of Soils and Sediments*, *15*(4), 792–804. https://doi.org/10.1007/s11368-014-0964-7

Popa, N., & Visa, M. (2017). The synthesis, activation and characterization of charcoal powder for the removal of methylene blue and cadmium from wastewater. *Advanced Powder Technology*, *28*(8), 1866–1876. https://doi.org/10.1016/j.apt.2017.04.014

Puga, A. P., Abreu, C. A., Melo, L. C. A., & Beesley, L. (2015). Biochar application to a contaminated soil reduces the availability and plant uptake of zinc, lead and cadmium. *Journal of Environmental Management*, *159*, 86–93. https://doi.org/10.1016/j.jenvman.2015.05.036

Qambrani, N. A., Rahman, M. M., Won, S., Shim, S., & Ra, C. (2017). Biochar properties and eco-friendly applications for climate change mitigation, waste management, and wastewater treatment: A review. *Renewable and Sustainable Energy Reviews*, *79*, 255–273. https://doi.org/10.1016/j.rser.2017.05.057

Qi, X., Xu, X., Zhong, C., Jiang, T., Wei, W., & Song, X. (2018). Removal of Cadmium and Lead from Contaminated Soils Using Sophorolipids from Fermentation Culture of Starmerella bombicola CGMCC 1576 Fermentation. *International Journal of Environmental Research and Public Health*, *15*(11), 2334. https://doi.org/10.3390/ijerph15112334

Qian, K., Kumar, A., Zhang, H., Bellmer, D., & Huhnke, R. (2015). Recent advances in utilization of biochar. *Renewable and Sustainable Energy Reviews*, *42*, 1055–1064. https://doi.org/10.1016/j.rser.2014.10.074

Rajapaksha, A. U., Chen, S. S., Tsang, D. C. W., Zhang, M., Vithanage, M., Mandal, S., et al. (2016). Engineered/designer biochar for contaminant removal/immobilization from soil

781 and water: Potential and implication of biochar modification. *Chemosphere*, *148*, 276–
782 291. https://doi.org/10.1016/j.chemosphere.2016.01.043
783 Rasa, K., Heikkinen, J., Hannula, M., Arstila, K., Kulju, S., & Hyväluoma, J. (2018). How
784 and why does willow biochar increase a clay soil water retention capacity? *Biomass and*
785 *Bioenergy*, *119*(October), 346–353. https://doi.org/10.1016/j.biombioe.2018.10.004
786 Rashed, M. N. (2001). Lead removal from contaminated water using mineral adsorbents.
787 *Environmentalist*, *21*(3), 187–195. https://doi.org/10.1023/A:1017931404249
788 Reddy, K. R., Xie, T., & Dastgheibi, S. (2014). Evaluation of Biochar as a Potential Filter
789 Media for the Removal of Mixed Contaminants from Urban Storm Water Runoff.
790 *Journal of Environmental Engineering*, *140*(12), 04014043.
791 https://doi.org/10.1061/(ASCE)EE.1943-7870.0000872
792 Rollinson, A. N. (2016). Gasification reactor engineering approach to understanding the
793 formation of biochar properties. *Proceedings of the Royal Society A: Mathematical,*
794 *Physical and Engineering Sciences*, *472*(2192). https://doi.org/10.1098/rspa.2015.0841
795 Rosales, E., Meijide, J., Pazos, M., & Sanromán, M. A. (2017). Challenges and recent
796 advances in biochar as low-cost biosorbent: From batch assays to continuous-flow
797 systems. *Bioresource Technology*, *246*, 176–192.
798 https://doi.org/10.1016/j.biortech.2017.06.084
799 Safatian, F., Doago, Z., Torabbeigi, M., Rahmani Shams, H., & Ahadi, N. (2019). Lead ion
800 removal from water by hydroxyapatite nanostructures synthesized from egg sells with
801 microwave irradiation. *Applied Water Science*, *9*(4), 1–6. https://doi.org/10.1007/s13201-
802 019-0979-8
803 Schmidt, H. P., Kammann, C., Niggli, C., Evangelou, M. W. H., Mackie, K. A., & Abiven, S.
804 (2014). Biochar and biochar-compost as soil amendments to a vineyard soil: Influences
805 on plant growth, nutrient uptake, plant health and grape quality. *Agriculture, Ecosystems*

806 *and Environment*, *191*, 117–123. https://doi.org/10.1016/j.agee.2014.04.001
807 Sirini, P. (2002). *Ingegneria sanitaria-ambientale*. (McGraw Hill, Ed.).
808 https://www.libreriauniversitaria.it/ingegneria-sanitaria-ambientale-sirini-
809 piero/libro/9788838608971. Accessed 6 March 2019
810 Sivaraj, R., Namasivayam, C., & Kadirvelu, K. (2001). Orange peel as an adsorbent in the
811 removal of acid violet 17 (acid dye) from aqueous solutions. *Waste Management*, *17*(21),
812 105–110. https://doi.org/10.1016/S0956-053X(00)00076-3
813 Sohi, S. P., Krull, E., Lopez-Capel, E., & Bol, R. (2010). A Review of Biochar and Its Use
814 and Function in Soil. *Advances in Agronomy*, *105*, 47–82. https://doi.org/10.1016/S0065-
815 2113(10)05002-9
816 Tan, Xiao fei, Liu, Y. guo, Gu, Y. ling, Xu, Y., Zeng, G. ming, Hu, X. jiang, et al. (2016).
817 Biochar-based nano-composites for the decontamination of wastewater: A review.
818 *Bioresource Technology*, *212*, 318–333. https://doi.org/10.1016/j.biortech.2016.04.093
819 Tan, Xiaofei, Liu, Y., Zeng, G., Wang, X., Hu, X., Gu, Y., & Yang, Z. (2015). Application of
820 biochar for the removal of pollutants from aqueous solutions. *Chemosphere*, *125*, 70–85.
821 https://doi.org/10.1016/j.chemosphere.2014.12.058
822 Tang, J., Zhu, W., Kookana, R., & Katayama, A. (2013). Characteristics of biochar and its
823 application in remediation of contaminated soil. *Journal of Bioscience and*
824 *Bioengineering*, *116*(6), 653–659. https://doi.org/10.1016/j.jbiosc.2013.05.035
825 Tatti, F., Papini, M. P., Raboni, M., & Viotti, P. (2016). Image analysis procedure for studying
826 Back-Diffusion phenomena from low-permeability layers in laboratory tests. *Scientific*
827 *Reports*, *6*(December 2015), 1–11. https://doi.org/10.1038/srep30400
828 Tatti, F., Petrangeli Papini, M., Torretta, V., Mancini, G., Boni, M. R., & Viotti, P. (2019).
829 Experimental and numerical evaluation of Groundwater Circulation Wells as a
830 remediation technology for persistent, low permeability contaminant source zones.

Journal of Contaminant Hydrology, *222*(February), 89–100. https://doi.org/10.1016/j.jconhyd.2019.03.001

Thomas, H. C. (1944). Heterogeneous Ion Exchange in a Flowing System. *Journal of the American Chemical Society*, *66*(10), 1664–1666. https://doi.org/10.1021/ja01238a017

Tripathi, M., Sahu, J. N., & Ganesan, P. (2016). Effect of process parameters on production of biochar from biomass waste through pyrolysis: A review. *Renewable and Sustainable Energy Reviews*, *55*, 467–481. https://doi.org/10.1016/j.rser.2015.10.122

Uchimiya, M., Lima, I. M., Thomas Klasson, K., Chang, S., Wartelle, L. H., & Rodgers, J. E. (2010). Immobilization of heavy metal ions (CuII, CdII, NiII, and PbII) by broiler litter-derived biochars in water and soil. *Journal of Agricultural and Food Chemistry*, *58*(9), 5538–5544. https://doi.org/10.1021/jf9044217

Uchimiya, M., Wartelle, L. H., Klasson, K. T., Fortier, C. A., & Lima, I. M. (2011). Influence of pyrolysis temperature on biochar property and function as a heavy metal sorbent in soil. *Journal of Agricultural and Food Chemistry*, *59*(6), 2501–2510. https://doi.org/10.1021/jf104206c

Vithanage, M., Herath, I., Joseph, S., Bundschuh, J., Bolan, N., Ok, Y. S., et al. (2017). Interaction of arsenic with biochar in soil and water: A critical review. *Carbon*, *113*, 219–230. https://doi.org/10.1016/j.carbon.2016.11.032

Wang, B., Gao, B., & Fang, J. (2017). Recent advances in engineered biochar productions and applications. *Critical Reviews in Environmental Science and Technology*, *47*(22), 2158–2207. https://doi.org/10.1080/10643389.2017.1418580

Wang, H., Gao, B., Wang, S., Fang, J., Xue, Y., & Yang, K. (2015). Removal of Pb(II), Cu(II), and Cd(II) from aqueous solutions by biochar derived from KMnO4treated hickory wood. *Bioresource Technology*, *197*, 356–362. https://doi.org/10.1016/j.biortech.2015.08.132

Wang, M., Zhu, Y., Cheng, L., Andserson, B., Zhao, X., Wang, D., & Ding, A. (2017). Review on utilization of biochar for metal-contaminated soil and sediment remediation. *Journal of Environmental Sciences (China)*, *63*, 156–173. https://doi.org/10.1016/j.jes.2017.08.004

Wani, A. L., Ara, A., & Usmani, J. A. (2015). Lead toxicity: a review. *Interdisciplinary Toxicology*, *8*(2), 55–64. https://doi.org/10.1515/intox-2015-0009

Weber, K., & Quicker, P. (2018). Properties of biochar. *Fuel*, *217*(September 2017), 240–261. https://doi.org/10.1016/j.fuel.2017.12.054

Weber, T. W., & Chakravorti, R. K. (1974). Pore and solid diffusion models for fixed-bed adsorbers. *AIChE Journal*, *20*(2), 228–238. https://doi.org/10.1002/aic.690200204

Wei, D., Li, B., Huang, H., Luo, L., Zhang, J., Yang, Y., et al. (2018). Biochar-based functional materials in the purification of agricultural wastewater: Fabrication, application and future research needs. *Chemosphere*, *197*, 165–180. https://doi.org/10.1016/j.chemosphere.2017.12.193

Yao, Z., You, S., Ge, T., & Wang, C. H. (2018). Biomass gasification for syngas and biochar co-production: Energy application and economic evaluation. *Applied Energy*, *209*(October 2017), 43–55. https://doi.org/10.1016/j.apenergy.2017.10.077

Yargicoglu, E. N., Sadasivam, B. Y., Reddy, K. R., & Spokas, K. (2015). Physical and chemical characterization of waste wood derived biochars. *Waste Management*, *36*, 256–268. https://doi.org/10.1016/j.wasman.2014.10.029

Yin, D., Wang, X., Chen, C., Peng, B., Tan, C., & Li, H. (2016). Varying effect of biochar on Cd, Pb and As mobility in a multi-metal contaminated paddy soil. *Chemosphere*, *152*, 196–206. https://doi.org/10.1016/j.chemosphere.2016.01.044

Yoon, Y. H., & Nelson, J. H. (1984). Application of Gas Adsorption Kinetics I. A Theoretical Model for Respirator Cartridge Service Life. *American Industrial Hygiene Association*

Journal, *45*(8), 509–516. https://doi.org/10.1080/15298668491400197

Zhang, Y., Chen, T., Liao, Y., Reid, B. J., Chi, H., Hou, Y., & Cai, C. (2016). Modest amendment of sewage sludge biochar to reduce the accumulation of cadmium into rice(Oryza sativa L.): A field study. *Environmental Pollution*, *216*, 819–825. https://doi.org/10.1016/j.envpol.2016.06.053